Taylor Neil Hughes

A Metabolomics Driven

Investigation of Polyamine

Metabolism

During Adipogenesis

A Metabolomics Driven Investigation of Polyamine Metabolism during
Adipogenesis

by

Taylor Neil Hughes

A project submitted to

Oregon State University

College of Agricultural Sciences

In partial fulfillment of

the requirements for the degree of

Baccalaureate of Science in BioResource Research

May 15th, 2015

Acknowledgements

I would like to extend a sincere thank you to Dr. Jan F. Stevens for his mentorship over the last few years as he gave me the great opportunity to work in his lab since the summer of 2013. I also owe a large thank you to Dr. Jay Kirkwood, who worked with me my first summer in the lab, made me familiar with many facets of a laboratory setting, and gave me the initial spark needed to start my project. Thank you, Dr. Cristobal Miranda for helping me with my cell culture experiments. I am also deeply indebted to Dr. Jaewoo Choi for helping run my samples in the mass spectrometry facility and processing my metabolomics data; this project would not have been successful without his expertise.

Linus Pauling Institute and
The Department of Pharmaceutical Sciences
Oregon State University, Corvallis, Oregon, U.S.A.

Table of Contents

List of Figures

List of Abbreviations

Acrolein	ACR
Arachidonoyl ethanolamide	AEA
Body mass index	BMI
Cannabinoid receptor 1	CB1
Cannabinoid receptor 2	CB2
Carboxyethyl mercapturic acid	CEMA
Differentiation medium	DM
Dulbecco's Modified Eagle Medium	DMEM
Endocannabinoids	ECBs
Fatty acid amide hydrolase	FAAH
Fatty acid amides	FAAs
Fetal bovine serum	FBS
Glutathione	GSH
Hank's Balanced Salt Solution	HBSS
Hydrogen Peroxide	H_2O_2
Hydroxylated major metabolite of GSH-ACR	GSH-HP
Hydroxypropyl mercapturic acid	HPMA
Isobutylmethylxanthine	IBMX
Liquid chromatography quadrupole time of flight tandem mass spectrometry	LC-QToF MS/MS
Mass-to-charge ratio	*m/z*
Parts-per million	ppm

List of Abbreviations (continued)

Peroxisome proliferator-activated receptor gamma$\qquad$PPAR-γ

Polyamine oxidase$\qquad$$PAO_x$

Reactive oxygen species$\qquad$ROS

Spermidine/spermine N^1-acetyltransferase$\qquad$SSAT

White adipose tissue$\qquad$WAT

Obesity. Throughout the world the scientific community has observed an increase in the prevalence of obesity and diabetes. In the United States alone, obesity has reached epidemic like proportions. The American Heart Association identified an estimated 23.9 million children ages 2 to 19 as being overweight or obese, 33% of boys and 30% of girls. Additionally, they stated as of 2013 an approximate 154.7 million adults 20 years or older suffered from the same condition, totaling 79.9 million men and 74.8 million women (Go et al., 2013). Obesity is achieved at the point where fat accumulation begins to exert deleterious effects on an organism. The human body accrues fat when there is an energy imbalance occurring, where caloric intake exceeds expenditure. Equipping one's self with effective means of reducing body fat alleviates all risk factors associated with the metabolic syndrome. For many people, since the accumulation of fat happens when intake exceeds expenditure, exercising to the point where expenditure exceeds intake is an attractive measure to reduce the degree of visceral obesity. However, due to large variations in the severity of obesity, exercise is not always feasible as a measure to reduce one's body mass index (BMI), or at least not until some body weight is lost. For this reason therapeutics can be used as a means to treat certain individuals

suffering from obesity and related ailments. Many anti-obesity drugs

used in the past have had undesirable side effects, and currently

there is a push to develop safer, nutraceutical agents, derived from

natural products (Colitti & Grasso, 2014).

Metabolic Syndrome. A cluster of risk factors that increase the risk

of developing cardiovascular disease characterizes the metabolic

syndrome. The prevalence of these cardiometabolic disorders

increases with the severity of obesity (Keller & Lemberg, 2003). The

conditions, which comprise metabolic syndrome, include visceral

obesity, dyslipidemia, insulin resistance, hypertension, chronic

inflammation, and thrombotic disorders that contribute to endothelial

dysfunction and, subsequently, accelerated atherosclerosis (Abella et

al., 2013). Relatively new knowledge of various neuroendocrine

interactions has revealed central obesity as a direct link to the

increasing occurrence of type II diabetes, cardiovascular disease, and

rheumatic diseases such as osteoarthritis and rheumatoid arthritis.

Adipose tissue. Fat tissue used to be regarded as a biological tissue

that functioned simply as an energy-storing medium. Fat tissue has

more recently been recognized as being a dynamic endocrine organ,

playing a key role at the crux of mechanisms and pathways involved

in longevity, inflammation, oxidative stress, and metabolic dysfunction

(Monickaraj et al., 2013). Describing adipose tissue as an endocrine
organ implies that it functions in biological signaling processes. The
signals emitted from fat tissue are bioactive substances that directly
influence insulin sensitivity and vascular injury. These bioactive
substances, which are factors that modify usual metabolic processes,
are commonly referred to as cytokines (Knights et al., 2014). They
have recently been given the more specific name of adipokines
(Proenca et al., 2014). Altered metabolic processes have been
identified as influencing the progression of metabolic syndrome
(Monickaraj et al., 2013). In the metabolic syndrome, accumulation of
excess fat causes harm to an organism, and increases stress. A
disturbance in the balance between the production of reactive oxygen
species (ROS) and antioxidant defenses achieves oxidative stress for
an individual.

Endocannabinoid system. Endocannabinoids (ECBs) are
neuromodulatory lipids that were initially of interest because of their
roles in the central nervous system (Butini et al., 2012). The ECB
system itself is a lipid signaling system within human tissues that is
mediated by G-protein coupled cannabinoid receptors. One class of
endogenous molecules that bind to these receptors is referred to as
fatty acid amides (FAAs). These receptors are responsible for binding
different ECBs and eliciting downstream signaling processes that

induce different physiological phenomena. Cannabinoid receptor 1 (CB1) and cannabinoid receptor 2 (CB2) have been isolated from mammalian tissues and their roles in facilitating different physiological effects are well studied. It has been reported that altered ECB system tone is characteristic in the pathologies of obesity and type 2 diabetes (Geurts et al., 2013). One important endocannabinoid is anandamide, also known as arachidonoyl ethanolamide (AEA). Originally studied for their central effects, such as regulation of pain, hunger, motility, and sleep, research on ECBs is shifting to investigate their role in peripheral tissue—controlling cell growth, death, and inflammation (Siegmund et al., 2006). Their diverse pharmacological activities and resultant effects may be explained in part by their diverse distribution in tissues (Pertwee et al., 2008). These receptors are of the same type bound by psychoactive molecules absorbed by ingesting cannabis. Cannabinoid receptors have not evolved due to human use of cannabis, however; instead, plant cannabinoids are agonists for receptors that the scientific community has termed—cannabinoid receptors. Rimonabant was used as an appetite suppression drug, working by way of inverse agonism of the CB1 receptor, but was eventually removed from the market due to undesirable side effects (Moreira et al., 2009). Inverse agonists produce effects opposite of their normal receptor bound ligands. If Rimonabant produced opposite effects than natural FAA ligands of the CB1, then binding of

the CB1 by endogenous FAAs would be expected to stimulate appetite.

The chief enzyme recognized to terminate AEA signaling is fatty acid amide hydrolase (FAAH), and thus this enzyme plays a key role in regulating these cellular processes. Previous studies show that primary hepatocytes expressing high levels of FAAH were resistant to AEA induced cell death, but primary hepatic stellate cells expressed low levels of FAAH and were more sensitive to AEA induced cell death (Siegmund et al., 2006). The hydrolysis of anandamide by FAAH was shown to reduce AEA-induced formation of the ROS hydrogen peroxide (H_2O_2) and ultimately cell death. It has been reported that other primary fatty acid amides, such as oleamide, are hydrolyzed by FAAH. Oleamide is a known agonist of the CB1 receptor and has been identified as a potent vasodilator dependent upon another G protein-coupled receptor (Hiley and Hoi, 2007). Components of the ECB system can be upregulated, in 2011 an increase in FAAH activity was reported in mature human adipose tissue of individuals with a high BMI (Cable et al., 2011).

Adipogenesis. Adipogenesis describes the physiological process by which precursor fat cells (preadipocytes) differentiate into mature adipocytes. This process is necessary for the formation of mature fat

tissue that can be used for energy storage. The differentiation-committed precursor cells are necessary for the formation of white adipose tissue (WAT), and the use of the 3T3-L1 cell line is one of the most commonly studied models of cell differentiation. ROS are produced soon after initiation of adipogenesis and are required for complete adipocyte differentiation. The regulatory role(s) of ROS during adipogenesis has been under intense investigation recently but still little is known. ROS have been reported to expedite mitotic clonal expansion and peroxisome proliferator-activated receptor gamma (PPAR-γ) expression during 3T3-L1 preadipocyte differentiation, but the source of ROS was not elucidated (Lee et al., 2009). PPAR-γ agonists, such as rosiglitazone, have been shown to stimulate adipogenesis and evoke weight gain (Amato et al., 2012). AEA induce ROS (Siegmund et al., 2005). Using the FAAH inhibitor URB597 should inhibit its hydrolytic activity, sustaining more AEA and ROS in the cell to facilitate adipogenesis. ROS, which can cause oxidative stress, may induce an adaptive stress response during which the cells upregulate the synthesis of antioxidants, such as glutathione (GSH). Polyamines are low molecular weight, polycationic molecules essential for a wide array of cellular processes. The polyamines synthesized in mammalian cells include putrescine, spermidine, and spermine, all derived from L-ornithine. Although low in relative abundance, these alkylamines have a number of important

13

functions, including their involvement in chromatin conformation, gene

expression, membrane stability, and ion channel regulation (Casero &

Marton, 2007). Additionally, the literature reports polyamines playing

a key role in embryonic development and cell proliferation. More

notably, as adipogenesis occurs throughout the lifetime of an

individual, spermidine was reported as being proadipogenic (Heby,

1981). It is known that differentiation is not solely induced by

spermidine but is dependent on other inducers, notably

isobutylmethylxanthine (IBMX) and insulin (Erwin et al., 1984). In

other words, spermidine itself is necessary, but not sufficient. Along

with ROS, the toxic compound acrolein (ACR) is produced as a

byproduct of polyamine oxidation (Tomitori et al., 2005). Kesinger et

al. showed in 2010 that THP-1 cells are capable of GSH-conjugation

of ACR as a detoxification mechanism, but this has not been shown in

adipose tissue (Kesinger et al., 2010).

The biochemical process paralleling adipogenesis is called *de

novo* lipogenesis, synthesizing palmitic acid from acetyl-CoA. This

notion was strongly supported when a group showed that key

lipogenic enzyme activities are upregulated during adipogenesis,

while acetate is being incorporated into triglycerides (Mackall et al.,

1976). During lipogenesis acetyl-coA is converted into fatty acids.

Three fatty acids are ultimately esterified with glycerol to form

triglycerides that make up the lipid droplets stored by mature adipocytes. *De novo* lipogenesis is at the root of the obesity epidemic because it is, in essence, how fat is made and stored.

Fat cells expand and shrink with a respective increase or decrease of BMI, but an individual does not have the fat cells their entire life. The fat cell pool of an individual is renewed as adipogenesis and adipocyte death occurs throughout ones lifetime (Arner et al., 2010). Several studies have elucidated that exogenous antioxidants inhibit adipogenesis and that exogenous pro-oxidants accelerate adipogenesis. In adipose tissue, polyamines exhibit insulin like effects, dependent upon H_2O_2 formation, stimulating glucose transport (Livingston et al., 1977). Insulin signaling is also thought to be partially dependent upon H_2O_2 formation (Goldstein et al., 2005).

The speculative premise of the partially H_2O_2-dependent hydrolytic activity of the FAAH enzyme suggests that regulating the activity of FAAH and its substrates may interrupt the process of fat storage. Hydrolyzing FAAs into their respective fatty acids terminates the cell signal for certain receptors involved in regulating physiological phenomena that are involved in energy homeostasis. Moreover, exploration and therapeutic exploitation of related pathways may be significant in alleviating features of obesity. Elucidating mechanisms

involved in endocannabinoid signaling that alter the adaptive stress response of living adipocytes, and discovering to what degree endogenously derived lipids are made by adipocytes during lipogenesis, would be relevant in helping create a global understanding of the biochemistry behind obesity. Additionally, understanding the role that FAAs play in adipogenesis would be a contribution not yet reported in the literature.

Metabolomics. Metabolomics is the measurement of products of biochemical pathways. Metabolites are small molecules chemically transformed by metabolic processes in a living system. Measuring the small molecules biotransformed in various pathways serves as a functional readout of cellular state. Whereas measured genes and proteins from genomic and proteomic experiments are subject to epigenetic regulation and post-translational modifications, respectively, metabolites are direct signatures of biochemical activity and are easier to correlate with phenotype. The functional readout from a metabolomics experiment comprises the metabolome. The metabolome's collection of small molecules produced by small cells offers a window for looking at how mechanistic biochemistry relates to cellular phenotype (Patti et al., 2012). The proposed cell culture experiment (in Materials and Methods), and metabolomics analyses to follow, should shine light on the knowledge gaps associated with

16

polyamine metabolism during adipocyte differentiation. Metabolomics

is a useful analysis, necessary for this experiment because when you

conduct a cell culture experiment in which you treat cells with different

chemicals, you want to be able to identify significant changes in

certain metabolites between the treatment groups. By identifying

major changes in a chemical product under a given a treatment, you

can use that information to illustrate a picture of a biochemical

pathway, and identify what is occurring inside the cells. We

hypothesize that treatment with exogenous spermidine increases

production of ROS and ACR byproducts during adipogenesis, also

inducing the adaptive stress response, subsequently increasing the

production of GSH and GSH-ACR adducts.

Materials and Methods

Cell culture. The cell culture experiments were performed using 3T3-

L1 cells acquired from ATCC (Manassas, VA, USA). This cell line is

frequently used to study adipogenesis and is sufficient for these cell

culture experiments because we too are exploiting proliferating

adipocytes. The fibroblasts were propagated in 75 cm^2 flasks

containing Dulbecco's Modified Eagle Medium (DMEM) purchased

from Life Technologies (Grand Island, NY, USA) with 10% fetal bovine

serum (FBS) from Atlanta Biologicals (Atlanta, Georgia, USA), 100 units/ml penicillin, 100 µg/ml streptomycin (Life Technologies), and 1 mM pyruvate. Once the preadipocytes became confluent in the flasks, they were passed and plated in 2 mL aliquots into Multiwell Primaria 6 well plates from Benton Dickinson Labware (Franklin Lakes, NJ) at a density of 50,000 cells/well. The cells were seeded in complete DMEM culture medium. Complete DMEM culture was prepared by the addition of 56.2 mL FBS and 5.62 mL of penicillin-streptomycin to 500 mL of DMEM with 1 mM pyruvate and 4 mM L-glutamine to give final concentrations of 10% FBS, 100 units/mL penicillin and 100 µg/ml streptomycin as above. Plated cells in culture media were incubated for 2 days at 37°C in CO_2 and grown to confluence. Two days postconfluency (designated day 0), the medium was aspirated to waste and 3 mL of differentiation medium (DM) was added per well. DM consists of complete DMEM culture medium with 0.5 mM IBMX, 0.5 µM dexamethasone, and 1 µg/mL insulin. IBMX and dexamethasone were purchased from Sigma Life Science (St. Louis, Mo, USA). After incubation for 2 days (Day 2) at 37°C in the CO_2 incubator, medium was aspirated to waste and 3 mL of complete DMEM culture medium was added to each remaining well. There were 5 different treatment groups in total. Three wells containing 1.00×10^6 cells per treatment group were analyzed once.

Chemical treatments were performed according to the following

protocol (Table 1):

Table 1. Cell Culture Protocol

Plate Number	Well Number	Treatment
1	1-3	50 µM Spermidine
	4-6	50 µM Spermidine + 5 µM URB597
2	7-9	5 µM URB597
	10-12	DMSO
3	13-15	Untreated

To determine the effects of these treatments on the metabolome of

differentiating 3T3-L1 cells, it was necessary to prepare stock

solutions with treatment chemicals. To prepare 1 mL of 5 mM

URB597 required dissolving 1.69 mg of URB597 purchased from

Cayman Chemical Company (Ann Arbor, MI, USA) in 1 mL of DMSO.

Weight of URB597 needed = (1 ml x 0.005 moles per mL)(338.4

g/mol) = 1.69 mg. The stock solution was filtered through a 0.2 µm

filter before use, then 3 µL of 5 mM URB597 was administered to the

designated wells with 3 mL of culture medium to reach a final

concentration of 5 µM. Preparation of 1 mL of 50 mM spermidine

stock solution was achieved by adding 7.26 mg of spermidine

purchased from Sigma Life Science (St. Louis, Mo, USA) to 1 mL of

deionized water. Weight of spermidine needed = (1 mL x 0.05

mmoles per mL)(145.25 g/mol) = 7.26 mg. The stock solution was filtered through a 0.2 µm filter before use, then 3 µL of 50 mM spermidine was administered to the designated wells with 3 mL of culture media to reach a final concentration of 50 µM. Commercial insulin from Sigma Life Sciences comes in a stock solution of 10 mg/mL. To control for DMSO vehicle used for URB597, wells 10-12 were treated with 3 µL of DMSO. The treated plates of cells were incubated at 37°C in a CO_2 incubator for another 2 days.

2 days post-treatment (Day 4), the cells of wells 1-15 were scraped for metabolite extraction. Wells 1-15 first had their media aspirated to waste well by well, one plate at a time. The cells were then washed once with 1 mL of warm Hanks Balanced Salt Solution (HBSS) acquired from Sigma Life Sciences, and then aspirated. Four hundred microliters of extraction solvent (50:50, MeOH:EtOH, v:v) chilled in a -80 °C freezer was added to each well, then covered with an adherent sticker that comes with each plate and placed in the -80 °C freezer. These steps of the metabolite extraction discussed so far should be carried out relatively quickly, approximately 2-4 minutes per cell plate, to ensure quenching of metabolism. After 4 hours at -80 °C to induce cell lysis, the plates were removed one at a time and each well was thoroughly scraped individually and the contents were transferred with a pipette to 1.5 mL centrifuge tubes. The sample

tubes with extracted metabolites were then centrifuged for 10 minutes at 15,000 x g at 4°C. Following centrifugation, the supernatants (cell lysates) were transferred to 1.5 mL glass vials and stored at -80 °C until liquid chromatography quadrupole time-of-flight tandem mass spectrometry (LC-QToF MS/MS) analysis. LC-QToF MS/MS based metabolomics analyses were carried out as previously described by the Stevens lab (Kirkwood et al., 2013a; Kirkwood et al., 2013b).

Metabolomics. Experiments were conducted according to an established method in the Stevens lab (Kirkwood et al., 2013a; 2013b). The general workflow first necessitates the isolation of metabolites from biological samples. Second, the samples are analyzed via LC-QToF MS/MS. Third, chromatographic peaks that changed between groups of samples were identified. Fourth, mass-to-charge ratio (m/z) values were used to search in metabolite databases for putative identifications. Lastly, the putative identifications are confirmed by comparing fragmentation patterns from tandem mass spectrometry spectra (MS/MS), and retention times, to that of standard compounds. This workflow varies whether performing targeted (quantification of specific metabolites in samples) or untargeted metabolomics (global metabolic profile of biological samples). Peakview software version 1.2 (Applied Biosystems, Waltham, MA, USA) was used to acquire retention times and peak

intensities for a targeted metabolomic approach for my 15 samples (5

treatments done in triplicate). The retention times and intensities

measured in the samples were exported to an Excel spreadsheet

where they could be compared to the retention times and intensities of

a 635 compound library (IROA Technologies, Bolton, MA) in which we

have in-house standards for. From there, the measured metabolites

were compared to the standard metabolites by difference in

theoretical *m/z* and measured *m/z*—expressed as error in parts-per

million (ppm). Metabolites with too large an error (> 5 ppm) were

then eliminated. Metabolites discovered via a targeted metabolomics

approach were aided by Peakview software. The software has a

function that suggests possible chemical formulas when an exact

mass is entered. The major metabolite of GSH-ACR conjugation

hydroxypropyl glutathione was created using ChemDraw (PerkinElmer

Inc., Waltham, MA, USA) and imported to peak view, giving us an

uncharged exact mass of 365.1257.

Results

FAAs measured in fully differentiated adipose tissue after exogenous

treatment with URB597 were not significantly different than those

measured in the untreated DMSO control group. Data obtained

regarding FAAs did not support nor disprove our hypothesis.

Additionally, acetylated polyamines were not detected in cell lysates.

The polyamines spermidine and spermine decreased with exogenous

spermidine treatment, with $\log_2$ fold change values of -0.56 and -1.13,

respectively (Figure 1). However, the polyamine putrescine was

observed to change by 1.49 $\log_2$ fold, and the p-value associated with

that change was less than 0.01, indicating high statistical significance.

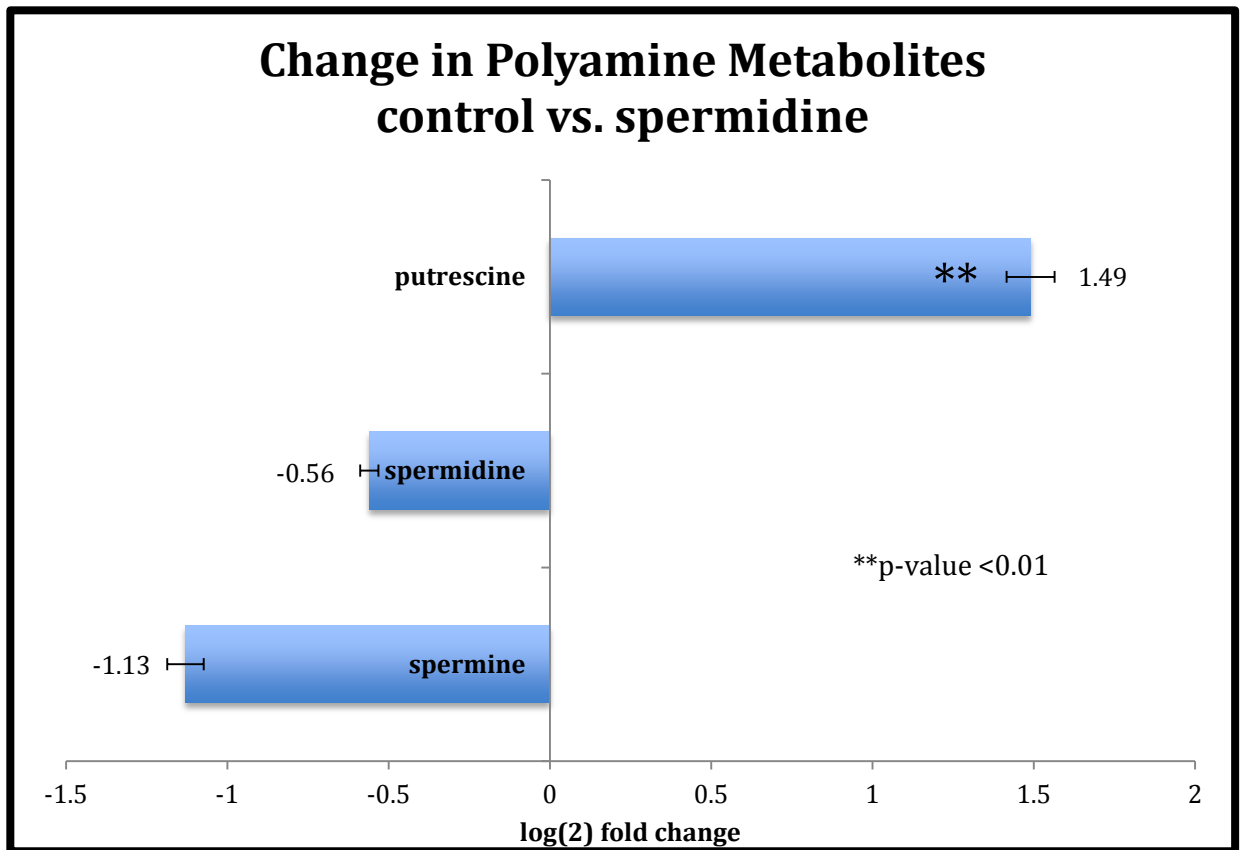**Change in Polyamine Metabolites control vs. spermidine**

Figure 1. The polyamines spermidine and spermine decreased in adipocytes treated with exogenous spermidine by -1.47 and -2.19 fold, respectively. Putrescine was observed to increase 2.82 fold after spermidine treatment. The p-value for putrescine from a paired t-test (n=3) was very low (< 0.01), indicating a statistically significant change.

After treatment with exogenous spermidine we observed a 2.67 fold increase (log2 fold change= 1.42) in the antioxidant GSH. Additionally we observed a 57.8 fold increase (log2 fold change= 5.86) in the GSH-ACR metabolite GSH-HP, each with a p-value < 0.01 (Figure 2). Also, the amino acids cysteine and glutamic acid, part of the tripeptide GSH, had log_2 fold changes of -0.317 and -0.029 respectively, which supports the idea of an induced adaptive stress response.
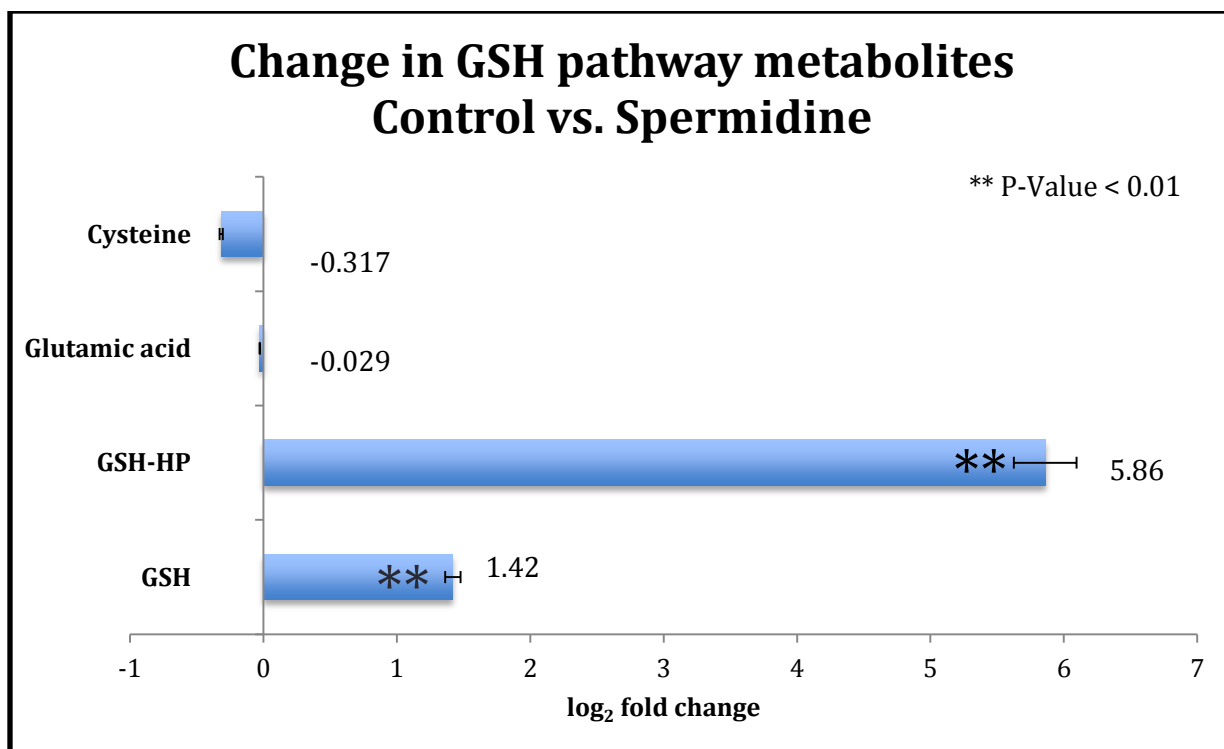
**Change in GSH pathway metabolites
Control vs. Spermidine**

** P-Value < 0.01

Cysteine -0.317

Glutamic acid -0.029

GSH-HP ** 5.86

GSH ** 1.42

$\log_2$ fold change

Figure 2. Acute increases in GSH (1.42 $\log_2$ fold change) and the glutathione-acrolein metabolite GSH-HP (5.86 $\log_2$ fold change) were observed following exogenous spermidine treatment. P-values for GSH-HP and GSH from paired t-tests (n=3) were both < 0.01, indicating changes with high statistical significance. The amino acids cysteine and glutamic acid decreased (-0.317 and -0.029 $\log_2$ fold change, respectively), supporting the idea of an induced adaptive stress response and upregulation of antioxidant defense.

GSH-HP was identified by positive ion TOF MS/MS scanning a range

of ions from *m/z* 40-1000. The spectra show that the parent

compound with a charged mass of 366.1 Da was eluted at 6.30

minutes. The highest intensity peak (base peak) for the MS/MS is for

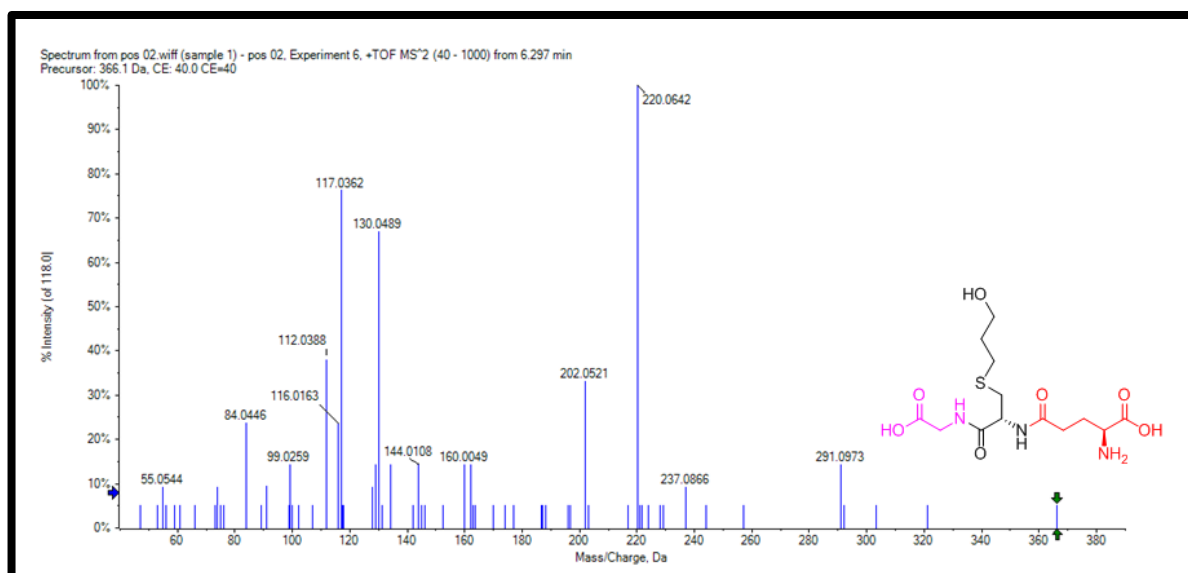a fragment with an accurate mass of 220.06 (Figure 3).

Figure 3. MS/MS spectra for GSH-HP. The GSH-HP ion with a charged mass of 366.1 had a retention time of 6.30 minutes. The base peak is representative of a fragment ion with an accurate mass of 220.06.

Discussion

Production of ACR *in vivo* can come as a byproduct of lipid peroxidation, glucose, protein, or polyamine metabolism (Stevens & Maier, 2008). The electrophilic nature of ACR enables it to adduct to DNA and protein, and the interaction has been reported to be involved in the development of certain types of cancers (Shields et al., 1995). The above-mentioned reason exemplifies why conjugation with GSH is an important detoxifying pathway in mammalian cells. Here we present evidence that in adipocytes, the formation of ACR is derived from spermidine. In this pathway, ACR and ROS are produced as byproducts of polyamine oxidation, and the ROS help facilitate the process of adipogenesis. Conjugation of ACR with GSH is well known, occurring via glutathione S-transferase mediated phase II

26

metabolism. Major metabolites of ACR that are excreted in human urine are products of the mercapturic acid pathway. They are hydroxypropyl mercapturic acid (HPMA) and carboxyethyl mercapturic acid (CEMA) (Lieberman et al., 1995). To become HPMA or CEMA, ACR derived from the breakdown of spermidine to putrescine must first be conjugated by the antioxidant GSH, creating GSH-ACR, which is further metabolized by aldehyde reduction into its corresponding alcohol, GSH-HP. To take part in the mercapturic acid pathway, GSH-ACR must have its glycine and glutamic acid residues cleaved off of its GSH moiety by the enzymes cysteineglycinase and γ-glutamyl-transpeptidase, leaving an unstable acrolein-cysteine intermediate, which then becomes N-acetylated by N-acetyltransferase (Yoshida et al., 2012). From there, two enzymatic reactions can occur. The N-acetylcysteine-ACR product can be converted to HPMA by aldehyde reductase, or to CEMA by aldehyde dehydrogenase (Figure 4).
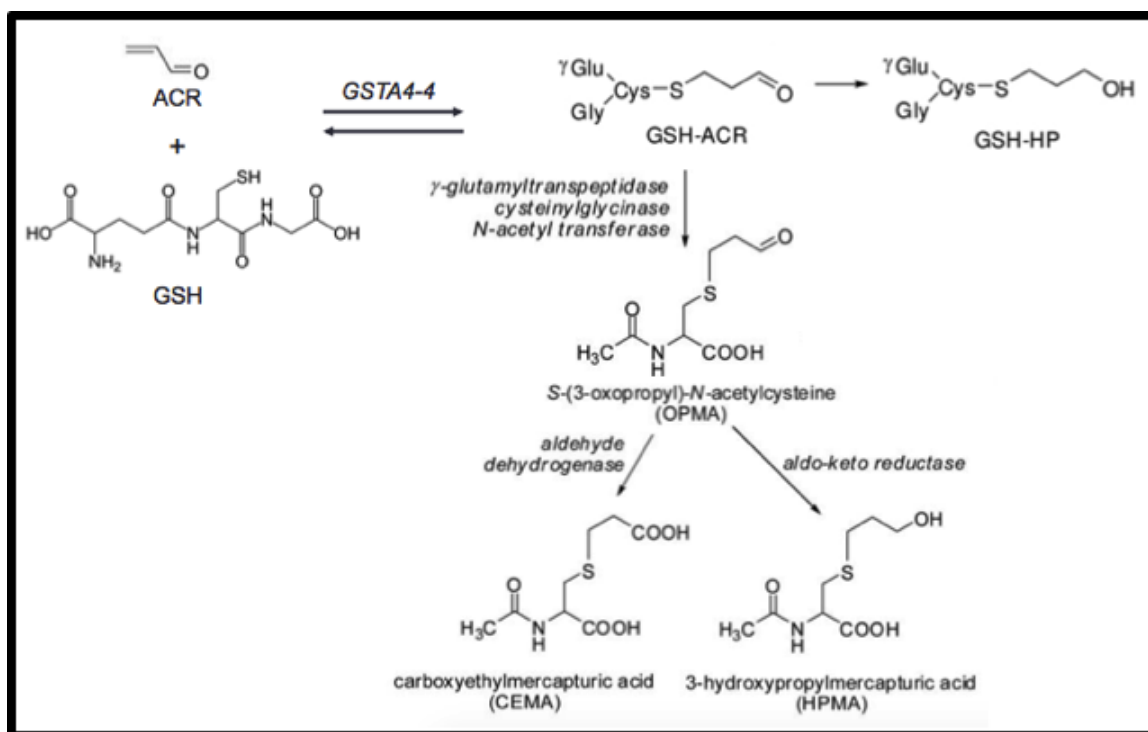
Figure 4. Metabolic pathway showing the formation of the glutathione-acrolein conjugates GSH-ACR and GSH-HP and subsequent degradation to mercapturic acid metabolites.

Peakview software gave us an MS/MS for the fragmentation of the compound (Figure 3) but there is no known fragmentation pattern reported in the literature for us to compare it to. Therefore, we dissociated the GSH-HP ion into fragment ions to see if we can suggest ions that match the m/z values given by the peak values from the MS/MS. The base peak shown in the MS/MS was for a fragment with a mass of 220.06. We suggest a mechanism for the formation of this ion, via a Mclafferty Rearrangement of GSH-HP (Figure 5). The Mclafferty Rearrangement is observed in mass spectrometry and is a characteristic fragmentation for ions with a carbonyl group that has at least one hydrogen atom attached to the gamma carbon.
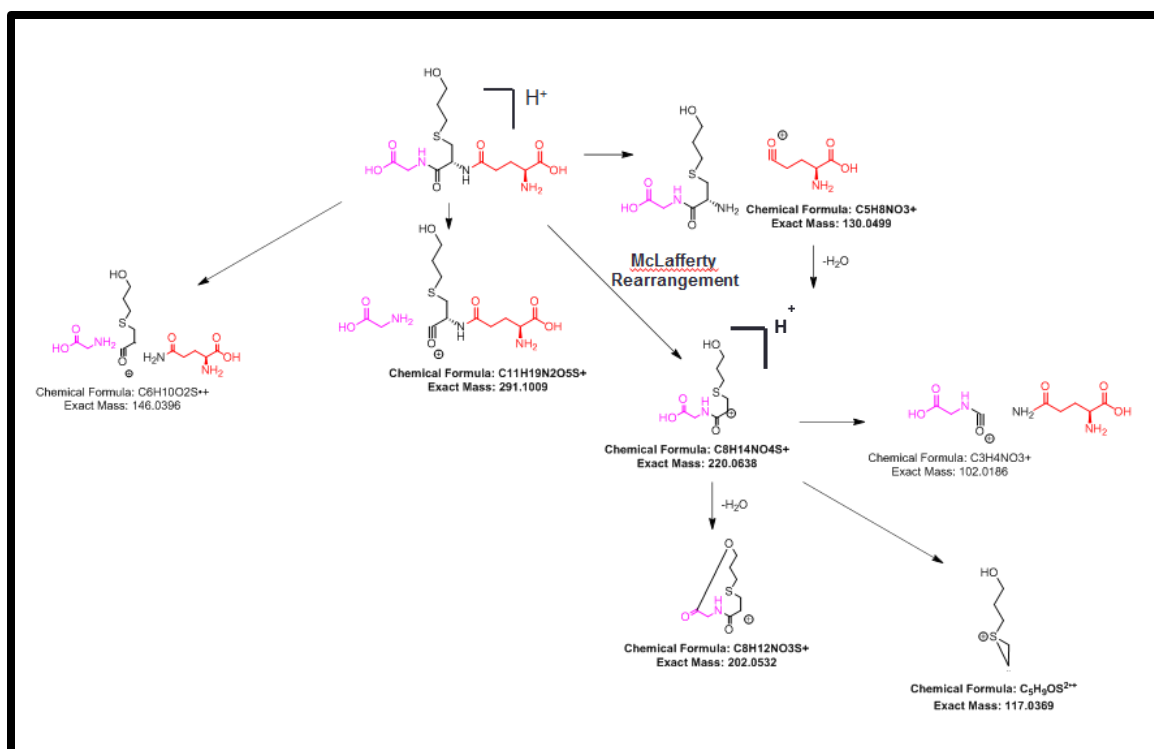
Figure 5. Proposed fragmentation pattern of GSH-HP. We suggest that the base peak of 220.0638 is formed via a McLafferty Rearrangement of GSH-HP. The rearrangement is a characteristic of molecular ions with a carbonyl group owning at least one gamma hydrogen.

Detection of GSH-HP, the major metabolite of GSH-ACR, shows that fat cells are capable of GSH conjugation of ACR and subsequent phase I metabolism of the GSH-ACR metabolite. This process occurs during adipogenesis and is upregulated with treatment of exogenous spermidine. GSH-HP originates from ACR. Levels of spermidine were shown to decrease after exogenous treatment with the compound itself. Its decrease in abundance reflects the fact that levels of putrescine were significantly increased in the cells, as spermidine is used as a substrate to synthesize putrescine.
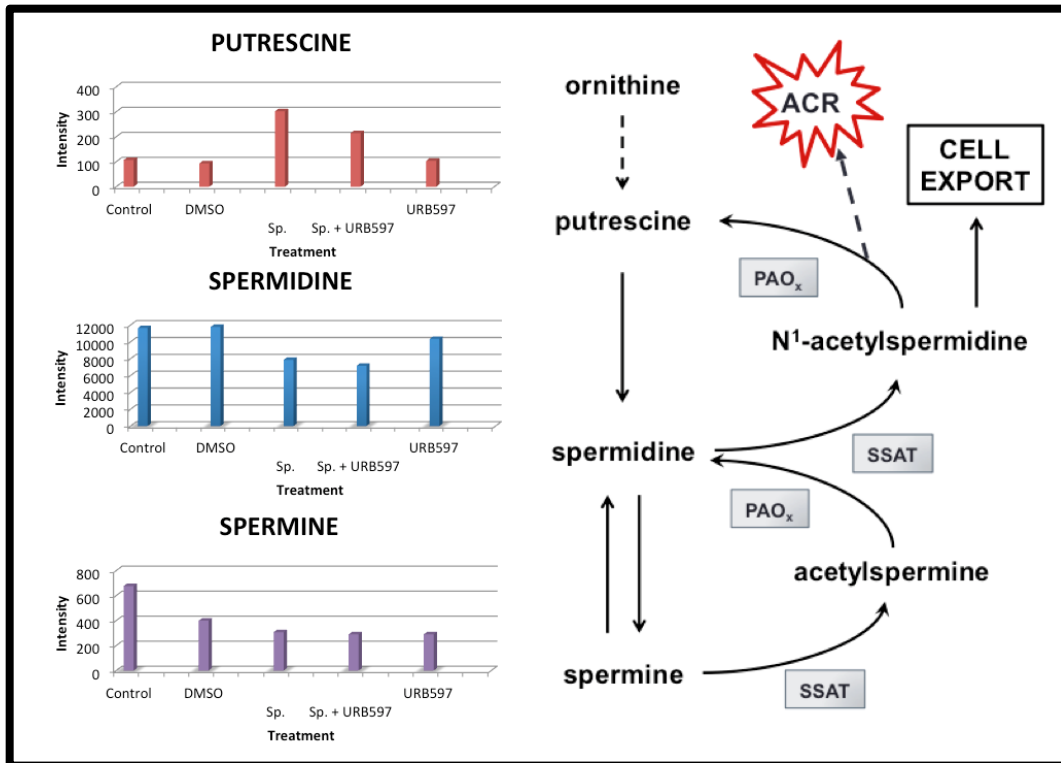
29

Figure 6. Measured intensities of small molecules involved in polyamine metabolism from targeted metabolomics analysis. This figure shows enzymes responsible for polyamine metabolism, and the creation of toxic ACR. Note: ornithine and acetylated polyamines were not detected.

A variety of enzymes are at play during metabolism, including spermidine/spermine N^1-acetyltransferase (SSAT) and polyamine oxidase (PAO_x); SSAT is normally expressed in low amounts in cells, but it is induced by stimuli such as polyamines (Mandal et al., 2013). It makes sense for the abundance of putrescine to increase since breakdown of spermidine to putrescine is a step where ACR is created. The aminoaldehyde products from enzymatic reactions of polyamine oxidase with spermine and spermidine spontaneously react to create ACR (Sakata et al., 2003). As stated in the results, acetylated polyamines were not detected in cell lysates, which is

expected as they are quickly transported out of the cell by the putative

diamine exporter (Gerner & Meyskens, 2004). It is the combination of

SSAT and PAO_x that work together to acetylate and oxidize

polyamines (Gerner & Meyskens, 2004; Wallace et al., 2003). We

show that through these oxidation reactions the essential ROS, H_2O_2,

is produced helping facilitate complete adipocyte differentiation.

Additionally, the important signaling molecule H_2O_2 is produced

concomitantly with the toxic compound ACR, but the cellular stress

events induce an adaptive stress response during which antioxidant

defense is upregulated by increased formation of GSH. Our findings

indicate that within the mercapturic acid pathway, conjugation of ACR

with GSH is a prevalent detoxification mechanism occurring in mature

adipose tissue.

References

1. Abella, V., Scotece, M., Conde, J., López, V., Lazzaro, V., Pino, J., et al. (2014). Adipokines, Metabolic Syndrome and Rheumatic Diseases. _J Immunol Res, 2014_, 343746.

2. Amato, A. A., Rajagopalan, S., Lin, J. Z., Carvalho, B. M., Figueira, A. C., Lu, J., et al. (2012). GQ-16, a novel peroxisome proliferator-activated receptor γ (PPARγ) ligand, promotes insulin sensitization without weight gain. _J Biol Chem, 287_(33), 28169-28179.

3. Arner, E., Westermark, P. O., Spalding, K. L., Britton, T., Rydén, M., Frisén, J., et al. (2010). Adipocyte turnover: relevance to human adipose tissue morphology. _Diabetes, 59_(1), 105-109.

4. Butini, S., Brindisi, M., Gemma, S., Minetti, P., Cabri, W., Gallo, G., et al. (2012). Discovery of potent inhibitors of human and mouse fatty acid amide hydrolases. _J Med Chem, 55_(15), 6898-6915.

5. Cable, J. C., Tan, G. D., Alexander, S. P., & O'Sullivan, S. E. (2011). The activity of the endocannabinoid metabolising enzyme fatty acid amide hydrolase in subcutaneous adipocytes correlates with BMI in metabolically healthy humans. _Lipids Health Dis, 10_, 129.

6. Casero, R. A., & Marton, L. J. (2007). Targeting polyamine metabolism and function in cancer and other hyperproliferative diseases. _Nat Rev Drug Discov, 6_(5), 373-390.

7. Colitti, M., & Grasso, S. (2014). Nutraceuticals and regulation of adipocyte life: Premises or promises. _Biofactors_.

8. Erwin, B. G., Bethell, D. R., & Pegg, A. E. (1984). Role of polyamines in differentiation of 3T3-L1 fibroblasts into adipocytes. _Am J Physiol, 246_(3 Pt 1), C293-300.

9. Gerner, E. W., & Meyskens, F. L. (2004). Polyamines and cancer: old molecules, new understanding. _Nat Rev Cancer, 4_(10), 781-792.

10. Geurts, L., Muccioli, G. G., Delzenne, N. M., & Cani, P. D. (2013). Chronic endocannabinoid system stimulation induces muscle macrophage and lipid accumulation in type 2 diabetic mice independently of metabolic endotoxaemia. _PLoS One, 8_(2), e55963.

11. Go, A. S., Mozaffarian, D., Roger, V. L., Benjamin, E. J., Berry, J. D., Borden, W. B., et al. (2013). Heart disease and stroke statistics--2013 update: a report from the American Heart Association. *Circulation, 127*(1), e6-e245.

12. Goldstein, B. J., Mahadev, K., Wu, X., Zhu, L., & Motoshima, H. (2005). Role of insulin-induced reactive oxygen species in the insulin signaling pathway. *Antioxid Redox Signal, 7*(7-8), 1021-1031.

13. Heby, O. (1981). Role of polyamines in the control of cell proliferation and differentiation. *Differentiation, 19*(1), 1-20.

14. Hiley, C. R., & Hoi, P. M. (2007). Oleamide: a fatty acid amide signaling molecule in the cardiovascular system? *Cardiovasc Drug Rev, 25*(1), 46-60.

15. Keller, K. B., & Lemberg, L. (2003). Obesity and the metabolic syndrome. *Am J Crit Care, 12*(2), 167-170.

16. Kesinger, N. G., Langsdorf, B. L., Yokochi, A. F., Miranda, C. L., & Stevens, J. F. (2010). Formation of a vitamin C conjugate of acrolein and its paraoxonase-mediated conversion into 5,6,7,8-tetrahydroxy-4-oxooctanal. *Chem Res Toxicol, 23*(4), 836-844.

17. Kirkwood, J. S., Legette, L. L., Miranda, C. L., Jiang, Y., & Stevens, J. F. (2013). A metabolomics-driven elucidation of the anti-obesity mechanisms of xanthohumol. *J Biol Chem, 288*(26), 19000-19013.

18. Kirkwood, J. S., Maier, C., & Stevens, J. F. (2013). Simultaneous, untargeted metabolic profiling of polar and nonpolar metabolites by LC-Q-TOF mass spectrometry. *Curr Protoc Toxicol, Chapter 4*, Unit4.39.

19. Knights, A. J., Funnell, A. P., Pearson, R. C., Crossley, M., & Bell-Anderson, K. S. (2014). Adipokines and insulin action: A sensitive issue.*Adipocyte, 3*(2), 88-96.

20. Lee, H., Lee, Y. J., Choi, H., Ko, E. H., & Kim, J. W. (2009). Reactive oxygen species facilitate adipocyte differentiation by accelerating mitotic clonal expansion. *J Biol Chem, 284*(16), 10601-10609.

21. Lieberman, M. W., Barrios, R., Carter, B. Z., Habib, G. M., Lebovitz, R. M., Rajagopalan, S., et al. (1995). gamma-Glutamyl transpeptidase. What does the organization and expression of a multipromoter gene tell us about its functions? *Am J Pathol, 147*(5), 1175-1185.

22. Livingston, J. N., Gurny, P. A., & Lockwood, D. H. (1977). Insulin-like effects of polyamines in fat cells. Mediation by H2O2 formation. *J Biol Chem, 252*(2), 560-562.

23. Mackall, J. C., Student, A. K., Polakis, S. E., & Lane, M. D. (1976). Induction of lipogenesis during differentiation in a "preadipocyte" cell line. *J Biol Chem, 251*(20), 6462-6464.

24. Mandal, S., Mandal, A., Johansson, H. E., Orjalo, A. V., & Park, M. H. (2013). Depletion of cellular polyamines, spermidine and spermine, causes a total arrest in translation and growth in mammalian cells. *Proc Natl Acad Sci U S A, 110*(6), 2169-2174.

25. Monickaraj, F., Aravind, S., Nandhini, P., Prabu, P., Sathishkumar, C., Mohan, V., et al. (2013). Accelerated fat cell aging links oxidative stress and insulin resistance in adipocytes. *J Biosci, 38*(1), 113-122.

26. Moreira, F. A., & Crippa, J. A. (2009). The psychiatric side-effects of rimonabant. *Rev Bras Psiquiatr, 31*(2), 145-153.

27. Patti, G. J., Yanes, O., & Siuzdak, G. (2012). Innovation: Metabolomics: the apogee of the omics trilogy. *Nat Rev Mol Cell Biol, 13*(4), 263-269.

28. Pertwee, R. G. (2008). The diverse CB1 and CB2 receptor pharmacology of three plant cannabinoids: delta9-tetrahydrocannabinol, cannabidiol and delta9-tetrahydrocannabivarin. *Br J Pharmacol, 153*(2), 199-215.

29. Proenca, A. R., Sertie, R. A., Oliveira, A. C., Campaaa, A. B., Caminhotto, R. O., Chimin, P., et al. (2014). New concepts in white adipose tissue physiology. *Braz J Med Biol Res, 47*(3), 192-205.

30. Sakata, K., Kashiwagi, K., Sharmin, S., Ueda, S., & Igarashi, K. (2003). Acrolein produced from polyamines as one of the uraemic toxins. *Biochem Soc Trans, 31*(2), 371-374.

31. Shields, P. G., Xu, G. X., Blot, W. J., Fraumeni, J. F., Trivers, G. E., Pellizzari, E. D., et al. (1995). Mutagens from heated Chinese and U.S. cooking oils. *J Natl Cancer Inst, 87*(11), 836-841.

32. Siegmund, S. V., Seki, E., Osawa, Y., Uchinami, H., Cravatt, B. F., & Schwabe, R. F. (2006). Fatty acid amide hydrolase determines anandamide-induced cell death in the liver. *J Biol Chem, 281*(15), 10431-10438.

33. Siegmund, S. V., Uchinami, H., Osawa, Y., Brenner, D. A., & Schwabe, R. F. (2005). Anandamide induces necrosis in primary hepatic stellate cells.*Hepatology, 41*(5), 1085-1095.

34. Stevens, J. F., & Maier, C. S. (2008). Acrolein: sources, metabolism, and biomolecular interactions relevant to human health and disease. *Mol Nutr Food Res, 52*(1), 7-25.

35. Tomitori, H., Usui, T., Saeki, N., Ueda, S., Kase, H., Nishimura, K., et al. (2005). Polyamine oxidase and acrolein as novel biochemical markers for diagnosis of cerebral stroke. *Stroke, 36*(12), 2609-2613.

36. Wallace, H. M., Fraser, A. V., & Hughes, A. (2003). A perspective of polyamine metabolism. *Biochem J, 376*(Pt 1), 1-14.

37. Yoshida, M., Mikami, T., Higashi, K., Saiki, R., Mizoi, M., Fukuda, K., et al. (2012). Inverse correlation between stroke and urinary 3-hydroxypropyl mercapturic acid, an acrolein-glutathione metabolite. *Clin Chim Acta, 413*(7-8), 753-759.